Science of the Total Environment 698 (2020) 134133

Contents lists available at ScienceDirect

Science of the Total Environment

journal homepage: www.elsevier.com/locate/scitotenv

Combination of humic acid and clay reduce the ecotoxic effect of TiO_2 NPs: A combined physico-chemical and genetic study using zebrafish embryo

Krupa Kansara, Ashutosh Kumar *, Ajay S. Karakoti *

Biological & Life Sciences, School of Arts & Sciences, Ahmedabad University, Central Campus, Navrangpura, Ahmedabad 380009, Gujarat, India

HIGHLIGHTS

- TiO_2 NPs and TiO_2 NPs + Clay induce defects in dorso-ventral axis of zebrafish embryos.
- TiO_2 NPs and TiO_2 NPs + Clay altered the expression of neural network genes of zebrafish embryos.
- The combination of NOM showed protective effect on developing zebrafish embryos.
- HA and clay can act as nonhazardous agents to remove TiO_2 nanoparticle contamination

GRAPHICAL ABSTRACT

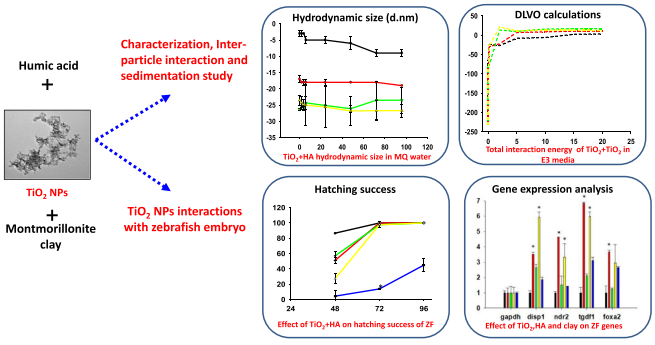

ARTICLE INFO

Article history:
Received 4 June 2019
Received in revised form 6 August 2019
Accepted 25 August 2019
Available online 29 August 2019

Editor: Daniel Wunderlin

Keywords:
Abiotic factors
Aggregation and sedimentation
Zebrafish embryos
Titanium dioxide nanoparticles
Developmental changes

ABSTRACT

The series of breakthroughs that have occurred within the realm of nanotechnology have been the source of several new products and technological interventions. One of the most salient examples in this regard is the widespread employment of titanium dioxide (TiO_2) nanoparticles across a range of consumer goods. Given that waste is generated at every stage of the consumer-product cycle (from production to disposal), many items with TiO_2 nanoparticles are likely to end up being discarded into water bodies. In order to understand the interaction of TiO_2 NPs with aquatic ecosystem, the ecological fate and toxicity of TiO_2 NPs was studied by exposing zebrafish embryos to a combination of abiotic factors (humic acid and clay) to assess its effect on the development of zebrafish embryos. The physiological changes were correlated with genetic marker analysis to holistically understand the effect on embryos development. Derjaguin–Landau–Verwey–Overbeek (DLVO) theory was used to analyze the interaction energy between TiO_2 NPs and natural organic matter (NOM) for understanding the aggregation behavior of engineered nanoparticles (ENPs) in media. The study revealed that combination of HA and clay stabilized TiO_2 NPs, compared to bare TiO_2 and HA or clay alone. TiO_2 NPs and TiO_2 NPs + Clay significantly altered the expression of genes involved in development of dorsoventral axis and neural network of zebrafish embryos. However, the presence of HA and HA + clay showed protective effect on zebrafish embryo development. The complete system analysis demonstrated the possible ameliorating effects of abiotic factors on the ecotoxicity of ENPs.

* Corresponding authors.
E-mail addresses: ashutosh.kumar@ahduni.edu.in (A. Kumar), ajay.karakoti@ahduni.edu.in (A.S. Karakoti).

https://doi.org/10.1016/j.scitotenv.2019.134133
0048-9697/

1. Introduction

Titanium dioxide nanoparticles (TiO_2 NPs) are one of the highly used and manufactured nanomaterials (Weir et al., 2012). TiO_2 NPs are used in various products like cosmetics, paints, food additives, pharmaceuticals, electronics and textiles as well as in construction and waste water treatment growth of low-cost and safer consumer products (Cheng et al., 2018). Interestingly, the production of TiO_2 nanoparticles has increased in United States from 3000 metric tons in the year 2002 to 260,000 metric tons in the year 2015 (Robichaud et al., 2009). Increasing production and usage of NPs can lead to its release in aquatic environment (Brun et al., 2018). It is estimated that up to 3–30% TiO_2 NPs will be dumped in aquatic environment (Keller and Lazareva, 2013). Hence, most of the organisms in aquatic environment will be exposed to TiO_2 NPs making it imperative to study and understand their effect on aquatic organisms.

The behavior and toxicity of NPs in aqueous environment is reported to be dependent on factors like pH, ionic strength, and types of salts, biotic and abiotic factors as well as their intrinsic properties like shape, size and crystalline form (Domingos et al., 2009a; Filho Jde et al., 2014; French et al., 2009; Gupta et al., 2017; Keller et al., 2010; Renieri et al., 2017). The basic studies related to the behavior and impacts of TiO_2 NPs in different environmental conditions have been reported previously (Faria et al., 2014; Guo et al., 2019; Romanello and Fidalgo de Cortalezzi, 2013; Sajjadi et al., 2013). The most common P25 TiO_2 NPs exhibited malformations in zebrafish embryos at 10 g/L with illumination and daily water exchanges for 23 days (Bar-Ilan et al., 2013). A recent study also reported the toxicity of bare P25 TiO_2 NPs on marine algae *Dunaliella salina* (Bhuvaneshwari et al., 2018). Previous studies about the effects of TiO_2 NPs on Artemia showed that higher concentrations (LC50 > 100 mg/L) and longer exposure duration caused mortality in both nauplii and adults (Ates et al., 2013). The effect of natural organic matter (NOM) on NPs was studied by Domingos et al. (Domingos et al., 2009b). These studies reported that, in presence of Suwannee River Fulvic Acid (2.5 mg/L), TiO_2 NPs showed high stability (Domingos et al., 2009b). It is usually hypothesized that abiotic factors like humic acid (HA) and clay minerals affect the stability of NPs and thus their resultant uptake and toxicity. HA is omnipresent in the environment (Hajdú et al., 2009) and is adsorbed on the NPs in aquatic systems altering their charge and resulting fate (Buffle et al., 1998). It was also reported that NOM can displace the original capping on NPs forming a protein corona like structure (Gupta et al., 2019; Mahmoudi et al., 2011; Radniecki et al., 2011). Clay minerals are abundant in aquatic environment and forms 30% of the total particulate colloidal matters available in environment (Wilkinson et al., 1997). Montmorillonite clay is an industrial silicate clay material used widely due to its large surface area, high swelling and high cation exchange capacity (Devi et al., 2015; Levard et al., 2013; Wang et al., 2015; Zhou et al., 2012). Clay minerals are known for altering the fate of NPs by agglomerating along with NPs.

Zebrafish (*Danio rerio*), a freshwater fish is extensively used as a research model due to its 70% gene similarity to that of humans, its transparent embryos that allows visualization of all the internal structures of the growing embryo, and also its ability to produce hundreds of offsprings in an interval of a week, its completely known genome and its easy maintenance (Gupta et al., 2016a; Howe et al., 2013). Several studies have reported the toxicity of titania nanoparticles using zebrafish as a model system (George et al., 2011; Lin et al., 2013) Andre Nel's group has demonstrated the use of Zebra fish as a high throughput screening approach for assessing the toxicity of bare NPs (George et al., 2011; Lin et al., 2013). Thus far reported studies have either focused on ecotoxicity exerted by bare titania NPs or in different salts or in the presence of HA. Most of these studies have been restricted to the observation of developmental changes in the model organism and very few studies have correlated the developmental changes with the molecular and genetic level information.

The present study was conducted to investigate ecotoxicity of TiO_2 NPs in aquatic environment by exposing zebrafish embryos to a combination of two most common abiotic factors (humic acid and clay) and assessing the effect of these abiotic factors on the development of zebrafish embryos. The combined effect of TiO_2 NPs in presence of NOM and clay on developmental genes of zebrafish was also analyzed by real time PCR. A majority of the genes from nodal signaling and Hedgehog (Hh) signaling pathway were targeted in this study. The genetic level information was evaluated and correlated with the developmental changes upon exposure to abiotic factors alone or in combination. The agglomeration and sedimentation of TiO_2 NPs in various salts in presence of abiotic factors was also studied. The Derjaguin–Landau–Verwey–Overbeek (DLVO) theory was used to analyze the interaction energy between TiO_2 NPs in presence of NOM and clay alone for understanding the aggregation mechanism of NPs. This study uniquely analyzes the combined effect of NOM and clay on TiO_2 NPs and correlates the observational changes in zebrafish development with the genetic changes in zebrafish.

2. Materials and methods

2.1. Chemicals and materials

A mixed rutile and anatase phase TiO_2 NPs (Catalogue No. PL-TiO-10p-10g) was procured commercially from Reinste Nano Ventures Pvt. Ltd. (Noida, India). Monrmorillonite K10 powder (CAS No.1318-93-0) and methylcellulose was procured from Sigma Chemical Co. Ltd. (St. Louis, MO, USA). 2′,7′-Dichlorofluorescein diacetate (DCFDA) dye was procured from Himedia Pvt. Ltd. (Mumbai, India). Humic Acid and all other chemicals were analytical reagent grade and purchased from Himedia Pvt. Ltd. (Mumbai, India).

2.2. Zebrafish maintenance

Assam wild-type strain of zebrafish was purchased from local vendor and maintained in standard laboratory conditions mentioned by ZFIN (Zebrafish Information Network) which includes temperature (26–28 °C) and 14 h light/10 h dark cycle (Westerfield, 2007). To mimic the natural environment in water tank, fresh water was artificially prepared by dissolving 60 mg/L sea salt (Red Sea, India) in distilled water. Artificial water quality was routinely assessed by checking different parameters i.e. pH (6.8–7.4), conductivity (250–350 μS), TDS (220–320 mg/L), salinity (210–310 mg/L) and dissolved oxygen (>6 mg/L) using multi-parameter instrument (Model PCD 650, Eutech, India). Zebrafishes were fed by live artemia (*Brine shrimp*) thrice in a day. Zebrafish breeding was conducted in ratios of two males and three females in breeding chamber (Gupta et al., 2016a). Eggs were collected in egg water containing sterile petri plates and raised at 28.0 °C in BOD incubator (MIR -154, Panasonic, Japan). The embryos were transferred to E3 medium (5 mM NaCl, 0.17 mM KCl, 0.33 mM $CaCl_2$ and $MgSO_4$, pH 7.0–7.2) and used for the experiment.

2.3. Preparation and characterization of TiO_2 NPs, humic acid and clay suspension

TiO_2 NPs stock suspension (1 g/L) was prepared in filtered MilliQ water. The suspension was diluted from this stock solution to various concentrations (1–100 mg/L) in E3 media and Milli Q water. Hydrodynamic size and zeta potential of bare TiO_2 NPs (50 mg/L), TiO_2 NPs (50 mg/L) + HA (10 mg/L), TiO_2 NPs (50 mg/L) + Clay (10 mg/L) and TiO_2 NPs (50 mg/L) + HA (10 mg/L) + Clay (10 mg/L) were determined by dynamic light scattering (DLS) and phase analysis light scattering (PALS) using a Zeta-sizer Nano-ZS equipped with a 4.0 mW, 633 nm laser from 0 to 96 h in E3 media and MilliQ water. The actual size distribution was further validated by transmission electron microscopy (TEM) (JEM1400 plus, JEOL, Japan). The samples for TEM imaging

were prepared by placing a drop of NPs suspension on carbon coated copper grids and allowed to dry for 2–3 h in a vacuum desiccator. All samples for TEM imaging were taken from freshly prepared suspension of TiO_2 NPs in presence and absence of abiotic factors.

Humic acid stock suspension (1 g/L) was made by dispersing HA powder in sterile MilliQ water and allowed to settle overnight at room temperature. For the experiments, the working concentration (10 mg/L) was made by diluting the supernatant in respective media. Clay suspension was prepared by dispersing 10 g/L montmorillionites (powder form) in MilliQ water (Cai et al., 2014; Zhou et al., 2012). Briefly, montmorillionite suspension was mixed at 50 RPM for 2 h. The suspension was allowed to settle overnight at room temperature to obtain a stable suspension. The supernatant was collected and dried in a hot air oven at 60 °C. Clay stock suspension (1 g/L) was made and - working clay suspension (10 mg/L) was made from the stock. The stock suspension was prepared from the dried powder. The hydrodynamic size and zeta potential measurements of humic acid and clay suspension were conducted by dynamic light scattering (DLS/PALS; Zetasizer Nano-ZS, Model ZEN3600 equipped with 4.0 mW, 633 nm laser; Malvern UK). Characterization was conducted in eight groups:

Group 1: TiO_2 NPs (50 mg/L) suspended in MilliQ water.

Group 2: TiO_2 NPs (50 mg/L) in combination with humic acid (10 mg/L) in MilliQ.

Group 3: TiO_2 NPs (50 mg/L) in combination with clay suspension (10 mg/L) in MilliQ.

Group 4: TiO_2 NPs (50 mg/L) in combination with humic acid (10 mg/L) and clay suspension (10 mg/L) in MilliQ.

Group 5: TiO_2 NPs (50 mg/L) suspended in E3 medium.

Group 6: TiO_2 NPs (50 mg/L) in combination with humic acid (10 mg/L) in E3 medium.

Group 7: TiO_2 NPs (50 mg/L) in combination with clay suspension (10 mg/L) in E3 water.

Group 8: TiO_2 NPs (50 mg/L) in combination with humic acid (10 mg/L) and clay suspension (10 mg/L) in E3 medium.

Characterization of all groups were conducted in a time dependent manner (i.e. 0, 2, 4, 6, 24, 48, 72 and 96 h), parallel to the in vivo experiments. To measure overall surface charge on NPs the zeta potential was analyzed and hydrodynamic sizes were measured to evaluate the aggregation and stability of NPs.

2.4. Sedimentation studies

Sedimentation behavior was monitored by studying the changes in absorbance of TiO_2 NPs in the presence of NOM at different time points (0, 2, 4, 6, 8, 24 and 48 h). The bare TiO_2 NPs (50 mg/L), TiO_2 NPs (50 mg/L) + HA (10 mg/L), TiO_2 NPs (50 mg/L) + Clay (10 mg/L) and TiO_2 NPs (50 mg/L) + HA (10 mg/L) + Clay (10 mg/L) were used for the study. The absorbance was measured by taking 1 mL of NPs suspension with and without NOM (prepared in E3 media) in a quartz cuvette with 1 cm optical path length and recorded using UV–Vis spectroscopy at 320 nm. A breakthrough curve was plotted for A_t/A_0 at y-axis and time (h) at x-axis where A_0 is absorbance at initial time point and A_t is absorbance at specific time intervals. Sedimentation studies were conducted in E3 media only with 50 mg/L TiO_2 NPs dispersed in 10 mg/L each of HA, clay or their combination.

2.5. Analysis of particles interaction using DLVO theory

The interaction between NOM and NPs was analyzed by the classic Derjaguin–Landau–Verwey–Overbeek (DLVO) theory. DLVO theory explains the aggregation of NPs and it is based on attractive van der Waals (vdW) and repulsive electrostatic forces from the overlap of the electrical double layers (EDL) of interactive surfaces (Chen and Elimelech, 2006). The van der Waals interaction was calculated from the Eq. (1) (Elimelech et al., 2013).

$$V_A = -\frac{\mathrm{Aa1a2}}{\mathrm{6h(a1 + a2)}} \tag{1}$$

here, a_1 and a_2 is particle radius, h is the separation distance, and A is the Hamaker constant. The electrostatic interaction between two dissimilar spheres was calculated by Eq. (2),

$$V_R = 64\pi\frac{a1a2}{a1 + a2}\left(\frac{kT}{ze}\right)2\gamma1\gamma2\ \exp(-kh) \tag{2}$$

here z is the indifferent ion valence, e is the elementary charge, κ is the Debye length, and γ is a dimensionless function of the surface potential, defined as,

$$\gamma = \tanh\left(\frac{ze\varphi}{4kT}\right) \tag{3}$$

ψ is the surface charge, approximated by the zeta-potential of the particles.

$$\mathrm{E} = V_A + V_R \tag{4}$$

The final interaction energy is given by the sum of attractive and repulsive energy (Eq. (4)). The particle sizes used for interaction analysis were measured from the particle size analysis (Section 2.3) in E3 media. For the simplicity the aggregation between engineered TiO_2 NPs or their aggregates were analyzed and abiotic factors (HA, clay or their combinations) were considered a part of the medium and heteroaggregation between TiO_2 and abiotic factors or their combinations were not analyzed.

2.6. Eco toxicity experiments

In vivo experiments for toxicity studies were conducted by distributing 15 embryos per well in a six well plate (Corning, NY, USA). Volume in each well was made up to 5 mL. One well was designated as control in each group without any NPs exposure. The final concentration of TiO_2 NPs in each well was 1 mg/L, 10 mg/L, 50 mg/L and 100 mg/L. The suspension of HA and clay (10 mg/L) were prepared first and NPs were added later. Treatment groups were as follow:

Group A: E3 medium having TiO_2 NPs (1 mg/L, 10 mg/L, 50 mg/L, 100 mg/L).

Group B: E3 medium having TiO_2 NPs (1 mg/L, 10 mg/L, 50 mg/L, 100 mg/L) suspended with humic acid (10 mg/L).

Group C: E3 medium having TiO_2 NPs (1 mg/L, 10 mg/L, 50 mg/L, 100 mg/L) with clay suspension (10 mg/L).

Group D: E3 medium having TiO_2 NPs (1 mg/L, 10 mg/L, 50 mg/L, 100 mg/L) with humic acid (10 mg/L) and clay suspension (10 mg/L).

Toxicity for TiO_2 NPs in presence of humic acid and clay particles was evaluated by observing viability and malformations. After the treatment, the viability i.e. number of live embryos, were counted manually using a stereo-zoom microscope (Model CETI; Medline Scientific Ltd., Banglore, India) at various time points (0, 2, 4, 24, 48, 72 and 96 h post treatment). Morphological changes and hatching delay were also recorded for the same time points.

2.7. Reactive oxygen species (ROS) estimation

The generation of ROS in the larvae exposed to all 4 groups (TiO_2 NPs, TiO_2 NPs + HA, TiO_2 NPs + Clay and TiO_2 NPs + HA + Clay) at variable TiO_2 NPs concentrations (1 mg/L, 10 mg/L, 50 mg/L, 100 mg/L) along with humic acid (10 mg/L) and clay suspension (10 mg/L) until 48 h was measured using dichlorofluorescein-diacetate (DCFH-DA). This assay was carried out according to the protocol described by Deng et al. (2009). Briefly, 10 larvae were washed with cold PBS

(pH 7.4) twice and then homogenized in cold buffer (0.32 mM of sucrose, 20 mM of HEPES, 1 mM of $MgCl_2$, and 0.5 mM of phenylmethyl sulfonylfluoride at pH 7.4). The homogenate was centrifuged at 15,000 $\times g$ at 4 °C for 20 min, and the supernatant was transferred to new tubes for further experimentation. 20 μL of the homogenate were added to a 96-well plate and incubated at room temperature for 5 min, after which 100 μL of PBS (pH 7.4) and 8.3 μL of DCFH-DA stock solution (dissolved in DMSO, 10 mg/mL) were added to each well. The plate was incubated at 37 °C for 30 min. The fluorescence intensity was measured in SYNERGY-HT multiwall plate reader (Bio-Tek, USA) using Gen5 software. The ROS generation was expressed in fold change.

The level of ROS in zebrafish larvae was determined as described (Wu et al., 2011). Briefly, treated embryos 48 h (post treatment) was taken in 12 well plates (5 embryos/well). All embryos (larvae) were incubated in DCFDA in concentration of 20 μM for 2 h at room temperature in dark. After incubation embryos were washed with E3 medium and then images were taken using fluorescent microscope (Massarsky et al., 2013).

2.8. Total RNA isolation

In brief, 50 embryos were exposed to all 4 groups (TiO_2 NPs, TiO_2 NPs + HA, TiO_2 NPs + Clay and TiO_2 NPs + HA + Clay) with TiO_2 NPs (50 mg/L) along with humic acid (10 mg/L) and clay suspension (10 mg/L) until 96 h. Total RNA isolation was conducted by RNAeasy mini kit (Qiagen 74104). RNA yield and integrity were determined using the SYNERGY-HT multiwall plate reader (Bio-Tek, USA) using Gen5 software. Primer sequences are included in SI Table 5.

2.9. Gene expression analysis

First-strand cDNA synthesis was performed with total RNA isolated from 50 embryos per replicate with a Maxima First Strand cDNA Synthesis Kit (ThermoFisher Scientific, USA) as per the manufacturer's protocol. Real-time PCR was performed using cDNA from each replicate and gene-specific primers with a powerup™ sybr® green master mix (ThermoFisher Scientific, USA) in the Quantstudio 5 (ThermoFisher Scientific, USA) according to the manufacturer's protocol. The signal output for each gene was normalized to the level of glyceraldehyde 3-phosphate dehydrogenase (GAPDH) to generate a relative expression ratio. Three independent experiments were performed for each gene, and the fold changes were averaged for a given sample.

2.10. Statistical analysis

All the experiments were performed in triplicates, and the results were expressed as mean ± standard error (SE) mean. The statistical analysis was carried out using Sigma plot® 10.0 and GraphPad Prism® version 8.0.2.

3. Results and discussion

3.1. Characterization of TiO_2 NPs

The average crystallite size of TiO_2 NPs was determined by analyzing 150 particles using imageJ. The average crystallite size of TiO_2 NPs was 8.6 ± 3 nm (Fig. 1). It is evident from the TEM images that the medium did not influence the aggregation or the individual crystallite size of the nanoparticles. Minor differences in the aggregation cannot be ascribed to the medium alone as the drying of nanoparticles over the TEM grid also can result in minor aggregation differences. It was also observed that clay particles were not found along with aggregates of TiO_2 NPs, as reported in some previous studies, possibly because of the very low concentration of clay used in the current studies (Labille et al., 2015; Zhou et al., 2012).

The hydrodynamic diameter and surface zeta potential of TiO_2 NPs were measured using DLS in both MilliQ water and fish embryo medium (E3 medium) (Fig. 2A–D). The hydrodynamic diameter measured as a function of time of TiO_2 NPs varied from 237 ± 28 to 239 ± 28 nm in MilliQ water and from 2148 ± 328 to 2876 ± 317 nm in E3 medium during the 96 h duration (SI Tables 1 and 2). The zeta potential of the NPs was slightly below the stability range, at −23 mV in MilliQ water and ranged between −3 ± 1 mV and −9 ± 1 mV in E3 medium (SI Tables 3 and 4). An increase in the size and decrease in surface zeta potential of TiO_2 NPs in E3 medium as compare to MilliQ can be attributed to the increased ionic strength of the E3 medium (Fig. 2). Increase in ionic strength causes agglomeration of TiO_2 NPs due to the compression of the electrical double layer (Gupta et al., 2016b). It was observed that the TiO_2 NPs showed heavy agglomeration immediately upon addition of E3 media and continued to show further agglomeration till 96 h.

3.2. Effect of NOM on aggregation of TiO_2 NPs

The hydrodynamic diameter and zeta potential of TiO_2 NPs was measured as a function of time in presence of HA (10 mg/L) and clay (10 mg/L) to understand the dynamic interaction of TiO_2 NPs (50 mg/L) with natural organic matter (NOM) and clay. As compared to bare TiO_2 NPs, hydrodynamic diameter was smaller in presence of HA, clay and mixture of HA and clay at all-time points in MilliQ water. The hydrodynamic diameter was smaller in presence of HA and varied from 174 ± 6 nm at the start to 216 ± 19 nm over a period of 96 h with inconsistent variation. At near neutral pH, humic acid is reported to be negatively charged and can adsorb on the surface of NPs through the carboxyl and phenolic groups (Jayalath et al., 2018). Additionally, the phenolic and carboxylic groups of HA have also been reported to play an important role in stabilization the particles via OH/OOH deprotonation (de Melo et al., 2016; Lagaly and Ziesmer, 2003; Pertusatti and Prado, 2007). This is also evident from the zeta potential of TiO_2 NPs and increased interaction in presence of HA in MilliQ that showed higher negative values at all-time points. Addition of clay to TiO_2 NPs in MilliQ also showed hydrodynamic size less than that of pure TiO_2 NPs at all-time points and varied from 216 ± 14 nm to 197 ± 27 nm suggesting that clay reduced the inter particle TiO_2 - TiO_2 interaction thereby resulting in smaller hydrodynamic diameter. Even though the clay particles are larger in size, the low concentration and platelet geometry of clay did not result in skewing of DLS data to higher size in MilliQ water. The zeta potential of TiO_2 NPs in presence of clay also showed slightly higher values around −30 mV, ranging from −31 mV to −25 mV over the time period of 96 h. These values were slightly lower than TiO_2 NPs + HA but higher than pure TiO_2 NPs suggesting only marginally better stability than pure TiO_2 NPs in MilliQ. Clay particles are known to possess both positive and negative charges on different surfaces that do not change in MilliQ water which is deprived of free ions. In presence of both HA and clay, TiO_2 NPs showed hydrodynamic diameter intermediate of that in HA and in clay. The zeta potential values were however low in the initial stages (0 to 2 h) and only increased marginally (from −19 mV to −24 mV) over a period of time (4 to 48 h). This suggest an interaction between HA and clay especially the positive charges on clay and negative charge on HA that results in slightly lower zeta potential values.

The E3 media consists of a mixture of salts in high ionic strength that results in immediate destabilization of TiO_2 NPs as discussed earlier. Addition of HA did not seem to prevent the agglomeration though the hydrodynamic diameter was smaller (1852 nm) as compared to bare TiO_2 immediately upon addition of E3 media and gradually increased upon aging for 96 h to 2207 nm with slight variations. The zeta potential also showed slightly higher values of −17 mV immediately upon addition and the zeta potential values changed only marginally and stayed below the stability limit throughout the 96 h aging. Addition of clay had similar effect on the stabilization of TiO_2 NPs. It was found that the hydrodynamic diameter increased from 1875 nm to 2551 nm over

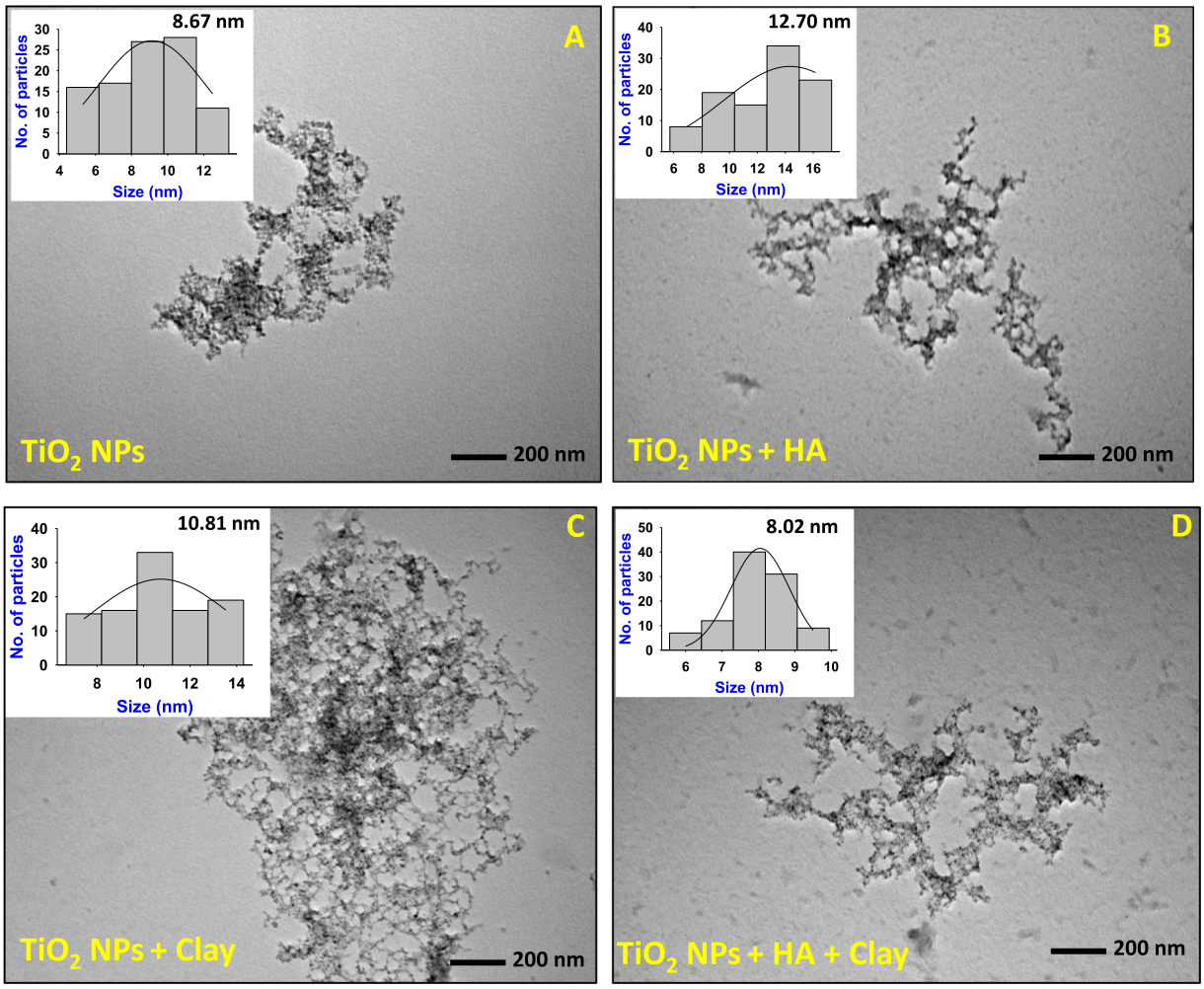

Fig. 1. TEM micrographs of (A) TiO_2 NPs (10 mg/L) (B) TiO_2 NPs (10 mg/L) + HA (5 mg/L) (C) TiO_2 NPs (10 mg/L) + Clay (5 mg/L) (D) TiO_2 NPs (10 mg/L) + HA (5 mg/L) + Clay (5 mg/L).

the period of 96 h aging though the intermediate time points showed a slow increase in agglomerate sizes with smaller aggregate sizes as compared to bare or HA stabilized TiO_2. The zeta potential of TiO_2 NPs in clay was highest among all combinations in E3 media at all time-points. This was reflected in reducing the heavy agglomeration observed for bare TiO_2 NPs and TiO_2 NPs + HA in E3 media. Even though it was expected that high ionic strength of E3 media may result in compression of electrical double layer of clay particles similar to TiO_2 NPs however the high zeta potential shows that destabilization of TiO_2 NPs by E3 medium was slowed down in presence of clay mineral. It is known that clay particles have plate like structure with patch wise charge on face and edges (Zhou et al., 2012). Thus even though both TiO_2 NPs and clay are negatively charged at pH 7.4; TiO_2 NPs can be absorbed on edges that have positive charges. Additionally, it has also been shown that the attachment efficiency of TiO_2 NPs on clay particles is a function of both pH and ionic strength and increases as pH and ionic strength increases (Loosli et al., 2013). Thus an increase in ionic strength leads to increase in attachment (or heteroagglomeration) of TiO_2 NPs and clay in E3 media thereby destabilizing TiO_2 NPs. This destabilization even though results in adsorption of TiO_2 over clay particles but prevents an immediate heavy agglomeration as seen for bare TiO_2 NPs at the concentration ranges analyzed in this study.

The hydrodynamic diameter and zeta potential of TiO_2 NPs + HA + Clay was found to stay between that of TiO_2 NPs + HA and TiO_2 NPs + Clay in E3 media. Thus the combined system of TiO_2 NPs with HA and clay showed higher negative zeta potential values and lower hydrodynamic size than only TiO_2 NPs or TiO_2 NPs + HA. It was also observed that the increase in hydrodynamic diameter over 96 h was slower increasing from 1222 nm initially to only 1381 nm after 96 h. Similarly, the zeta potential values varied between −23 mV to −26 mV depicting that the HA + Clay system provides higher stability upon aging the NPs in E3 media as compared to only HA or only clay.

3.3. Sedimentation of TiO_2 NPs exposed to NOM

The sedimentation curve of TiO_2 NPs with different NOM combination is shown in Fig. 3. The sedimentation of TiO_2 NPs in E3 medium was similar in presence and absence of abiotic factors. The ratio of absorbance decreased steeply initially and continued to decrease till 6 h, suggesting heavy agglomeration of bare titania NPs in E3 medium. The sedimentation rate slowed down with time in the next 48 h. The presence of HA or clay did not seem to influence the sedimentation rate of TiO_2 NPs significantly as all the combinations resulted in sizes higher than 1 μm and smaller zeta potential values. The lower concentrations (10 mg/L) of NOM have only partial influence on larger aggregates of TiO_2 NPs.

3.4. Inter-particle interactions

The DLVO theory was used to calculate the inter particle interaction energy for TiO_2 NPs at different separation distance. Inter-particle interaction in presence of HA and clay were calculated and compared with bare TiO_2 nanoparticles in E3 medium. The total interaction energy was plotted as a function of inter-particle separation to monitor the

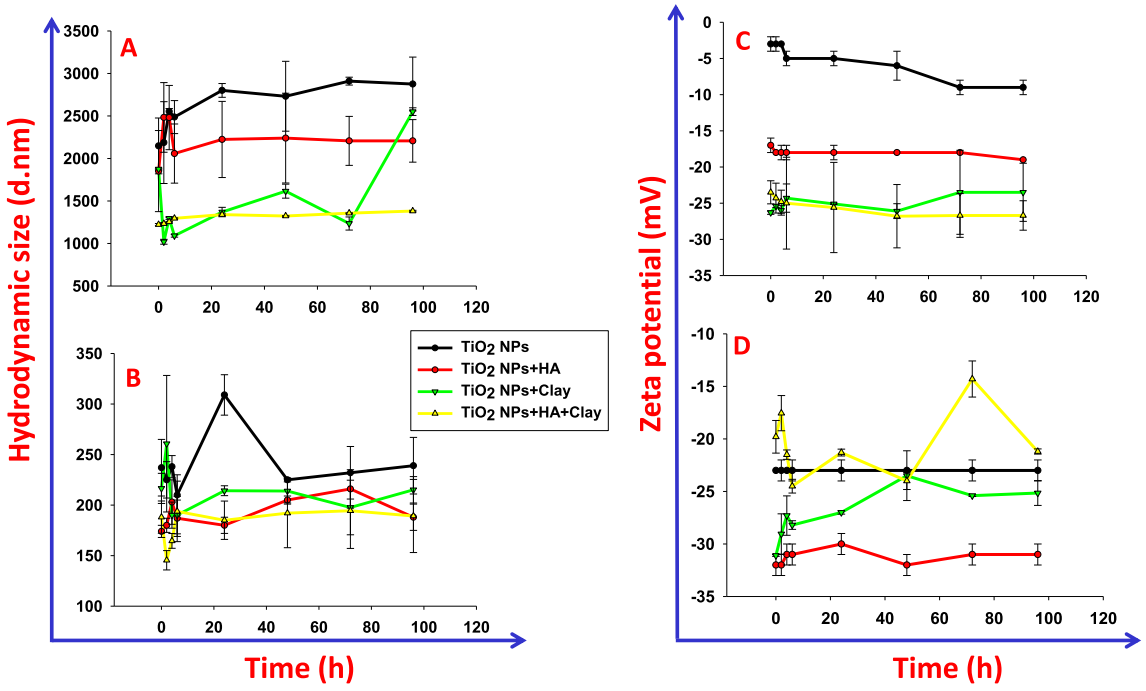

Fig. 2. Characterization of TiO_2 NPs (50 mg/L) in presence of Humic acid (10 mg/L), Clay (10 mg/L) and their combination in E3 media and MilliQ water by dynamic light scattering up to 96 h. (A) Hydrodynamic size in E3 media (B) Hydrodynamic size in MQ water (C) Zeta potential in E3 media (D) Zeta potential in MilliQ water.

stability of nanoparticles. High negative values at short distances indicate electrostatic repulsion of particles as they approach each other. Steeper curve in electrostatic repulsion region over short distances indicate low surface charge and thus low stability in media whereas shallow curves from highly charged particles show stability over medium to long range distance.

(a) **TiO_2 NPs in E3 media**: According to DLVO calculations, TiO_2 NPs showed two shallow repulsion energy minima at 12 nm and at 3 nm of 12 and 20 k_BT respectively immediately upon addition in E3 media. Two energy minima with gradual decrease in electrostatic repulsion energy points to repulsion between particles of different sizes and charge densities. A positive energy barrier at 20 k_BT was found at 3 nm upon aging for 48 to 96 h (Fig. 4A).

(b) **TiO_2 NPs with HA in E3 media**: The presence of HA did not alter the interaction energy plot drastically as reflected in DLS studies. However, the repulsion energy minima that was observed for longer distances for only TiO_2 NPs in E3 media disappeared and was restricted to <5 nm separation distance. The repulsion energy over short range distance was higher initially (at 0 to 24 h) as compared to only TiO_2 NPs. The energy barrier at 3 nm upon 48 h and 96 h aging was also present suggesting similarity in behavior probably due to higher ionic strength of E3 media and low concentration of HA (Fig. 4B).

(c) **TiO_2 NPs with clay in E3 media**: The interaction energy plot between TiO_2 NPs in presence of clay demonstrated that agglomeration proceeds rather freely between TiO_2 NPs. No significant changes were observed in electrostatic repulsion energy upon aging with slight increase in vdW attraction suggesting further agglomeration and increase in aggregation size upon aging probably aided by the heteroagglomeration of TiO_2 and clay (Fig. 4C).

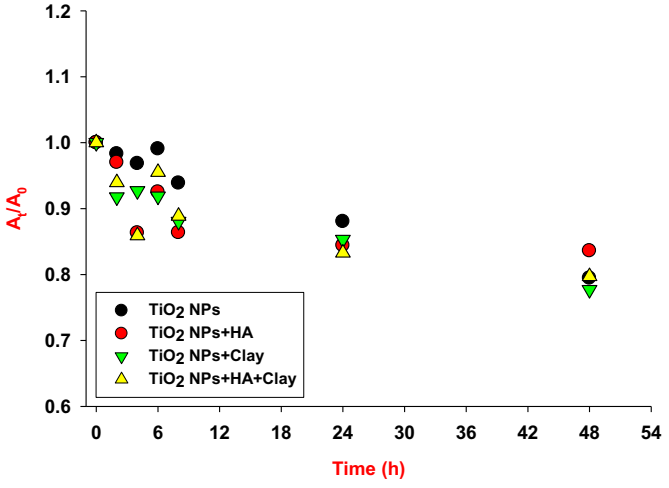

Fig. 3. Sedimentation behavior analysis of TiO_2 NPs (50 mg/L) in presence of Humic acid (10 mg/L), Clay (10 mg/L) and their combination in E3 media up to 48 h at neutral pH.

The DLVO interaction study shows that the high ionic strength of E3 media results in neutralization of charges and thus decreasing the contribution of electrostatic stabilization. The electrostatic energy was higher only at very small distances and the overall contribution to the stability (or aggregation) of nanoparticles at larger distances was primarily from van der Waals interaction.

3.5. Zebrafish embryos survival rate and hatching success

The zebrafish embryos survival rate was assessed by exposing them to TiO_2 NPs (at concentrations 1, 10, 50 and 100 mg/L) along with clay (10 mg/L) and humic acid (10 mg/L) from 0 to 96 hour post fertilization (hpf). It was observed that addition of clay and humic acid along with TiO_2 NPs altered the toxic effects exerted by TiO_2 NPs on zebrafish development. TiO_2 NPs induces mortality of the embryos, as 100% embryos were dead at exposure concentration 100 mg/L after 72 h (Fig. 5A). Earlier study showed that sub lethal levels of bare P25 TiO_2 NPs exposure caused alterations in larval swimming behaviors without affecting hatchability and survival of zebrafish (Chen et al., 2011b).

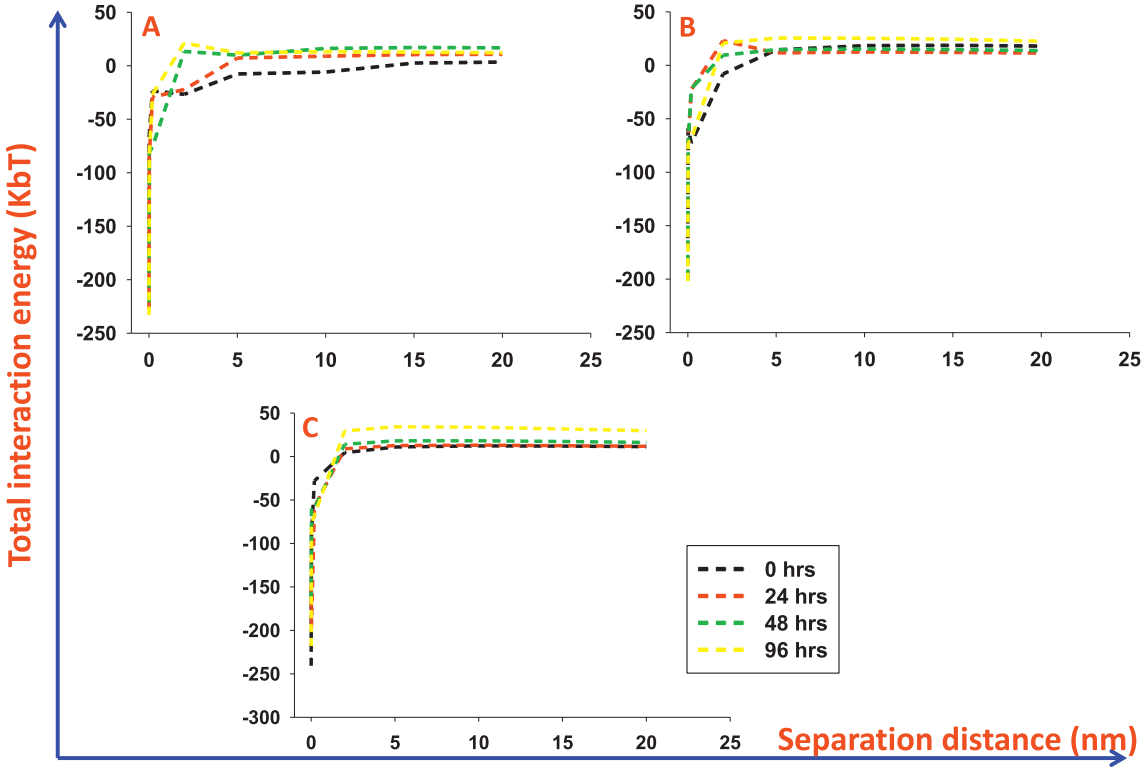

Fig. 4. Total interaction energy calculated by Derjaguin–Landau–Verwey–Overbeak (DLVO) in E3 media. (A) TiO_2 NPs (50 mg/L) and TiO_2 NPs (50 mg/L) (B) TiO_2 NPs (50 mg/L) and HA (10 mg/L) (C) TiO_2 NPs (50 mg/L) and Clay (10 mg/L) from 0 to 96 h at different separation distances.

However, the survival rate decreased to 20% with bare P25 TiO_2 NPs at 10 g/L in presence of illumination for 23 days (Bar-Ilan et al., 2013). However, the survival rate for TiO_2 NPs + HA, TiO_2 NPs + Clay, and TiO_2 NPs + HA + Clay after 72 h exposure was 75%, 33.3% and 80.7% respectively at same concentration, indicating the reduced mortality in presence of humic acid and mixture of HA and clay (Fig. 5B–D).

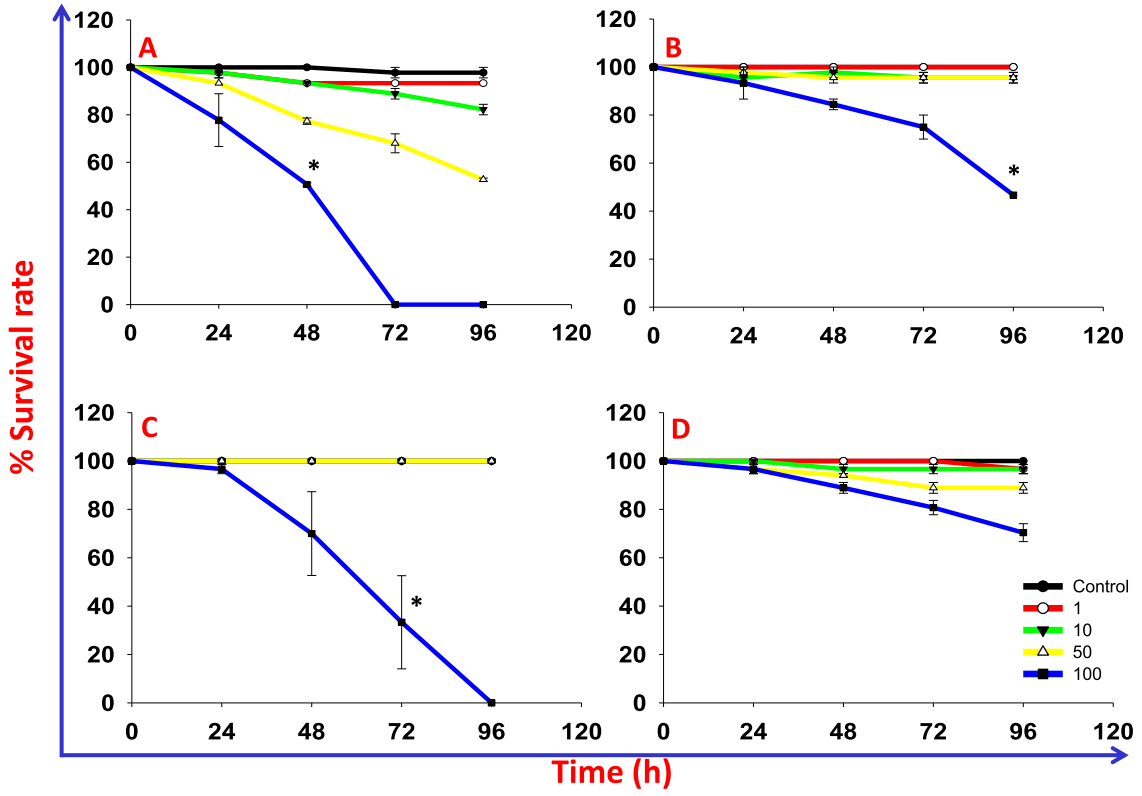

Fig. 5. Effects of humic acid (10 mg/L) and clay (10 mg/L) on the survival rate of zebrafish embryos after exposure to TiO_2 nanoparticles (1, 10, 50, 100 mg/L). (A) TiO_2 NPs (B) TiO_2 NPs + HA (C) TiO_2 NPs + Clay (D) TiO_2 NPs + HA + Clay. Data represent means±SEM of three independent experiments. $^{*}P < 0.05$, when compared with control.

This could possibly be due to the HA adsorption on the TiO_2 NPs, which forms a protective layer on NPs resulting in lower toxic effect of ENPs. HA also reduces the adhesion of TiO_2 NPs to embryo due to the increased electrostatic repulsion and steric repulsion and decreases the available surface area of TiO_2 NPs for the interaction with embryos that has increased the survival rate of embryos. Earlier studies have reported that in presence of HA, NPs exhibited less toxicity to non-vertebrate aquatic organisms (Chen et al., 2011a; Fabrega et al., 2009; Gao et al., 2009, 2012; Lee et al., 2011). However mixed results have been reported in terms of reduced survival in presence of NOM (Yang et al., 2013).

In the case of TiO_2 NPs + Clay treatment, the TiO_2 NPs are adsorbed on surface of clay particles resulting in the formation of heteroagglomerates, however this does not reduce the overall bioavailability of exposed TiO_2 NPs. Thus the possibility of TiO_2 NPs to be exposed to the organism and cross the outer protective layer of the embryo does not alter greatly. In presence of both humic acid and clay, bio-availabilities of free TiO_2 NPs are reduced by the presence of protective HA layer over the ENPs surface and hence they depict lesser toxicity. The chorion is the first physical barrier for NPs entry in early embryo development but it is unclear that how HA and clay play major role in transporting of NPs through chorion with volume of ~ 170 nm^3 (Cheng et al., 2007). The photographic representation of differences in survival rate and hatching success of zebrafish embryos exposed to different combinations of TiO_2 NPs with and without NOM up to 96 h is represented in Fig. 6.

The hatching was higher for HA, clay and HA + clay combinations as compared to only TiO_2 nanoparticles at 48 hpf in a concentration dependent manner. The hatching observed in embryos was 100%, 40%, 13% and 0% in combinations of TiO_2 NPs + HA + Clay, TiO_2 NPs + Clay, TiO_2 NPs + HA and TiO_2 NPs at concentration 100 mg/L after 72 hpf, respectively (Fig. 7A–D). The most apparent hatching success was observed in TiO_2 NPs + HA + Clay among all combinations (i.e. 1, 10, 50 and 100 mg/L) after 72 hpf (Fig. 7D). The hatching were observed in presence of HA and clay irrespective of the higher concentration of ENPs. The embryos exposed to TiO_2 NPs at 100 mg/L showed no hatching even after 96 hpf (Fig. 7A). This could possibly be due to the inhibition of enzymatic activity responsible for hatching by TiO_2 NPs (Bai et al., 2010; Ong et al., 2014). Moreover, HA and clay did not reverse the TiO_2 NPs (100 mg/L) potential to completely inhibit the hatching but hatching ability was increased (Fig. 7B–D).

Thus, present study observed that bare TiO_2 NPs had highest hatching delay at higher concentrations and lowest viability. However, the TiO_2 NPs grouped with clay and humic acid both, had lowest hatching delay and more viability, possibly due to the faster settling and humic acid coating on bare TiO_2 NPs. HA and clay are potential candidates to inhibit the toxicity of bare TiO_2 NPs regardless of their different mechanism.

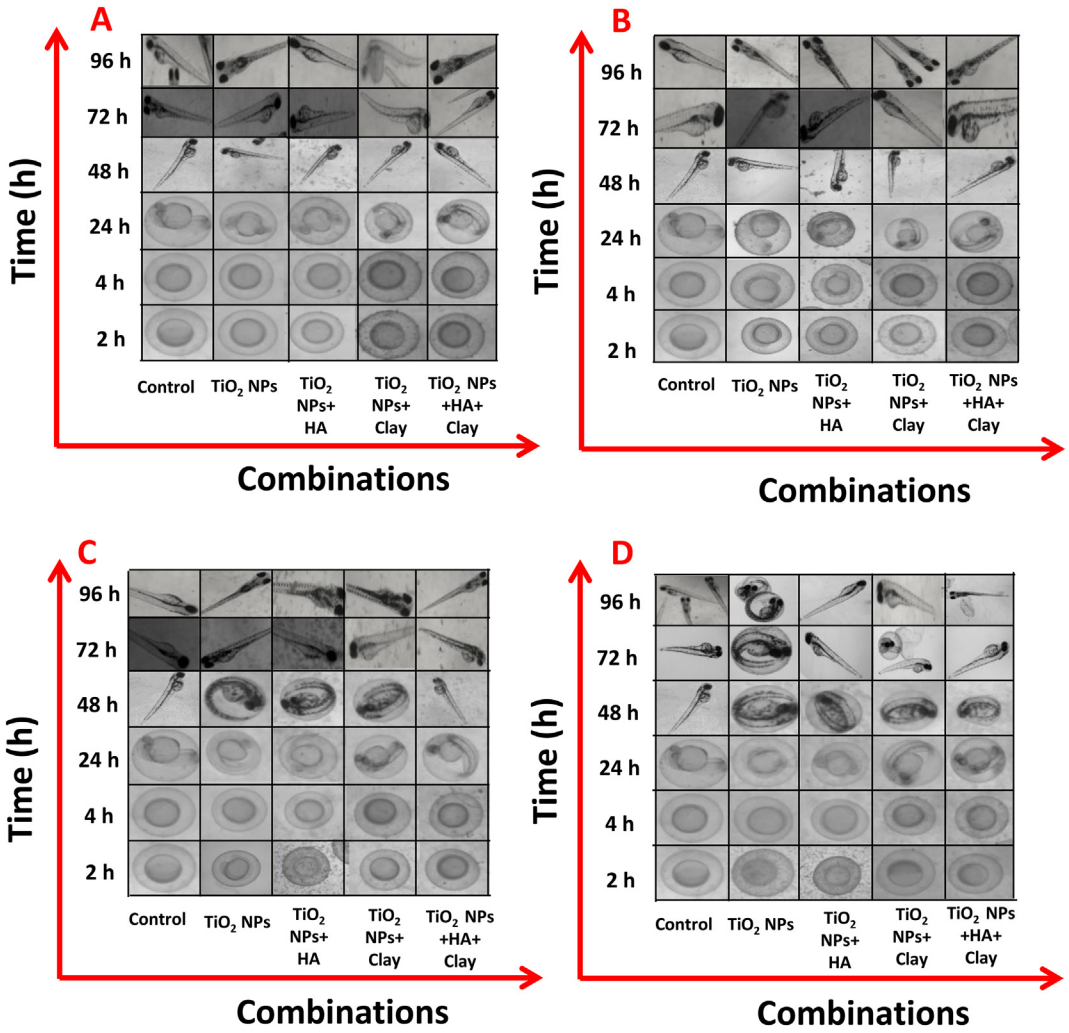

Fig. 6. Photographs representing the comparison of different combination of TiO_2 NPs (1, 10, 50, 100 mg/L) with humic acid (10 mg/L) and clay (10 mg/L) on the survival rate and hatching success. (A) 1 mg/L TiO_2 NPs (B) 10 mg/L TiO_2 NPs (C) 50 mg/L TiO_2 NPs (D) 100 mg/L TiO_2 NPs.

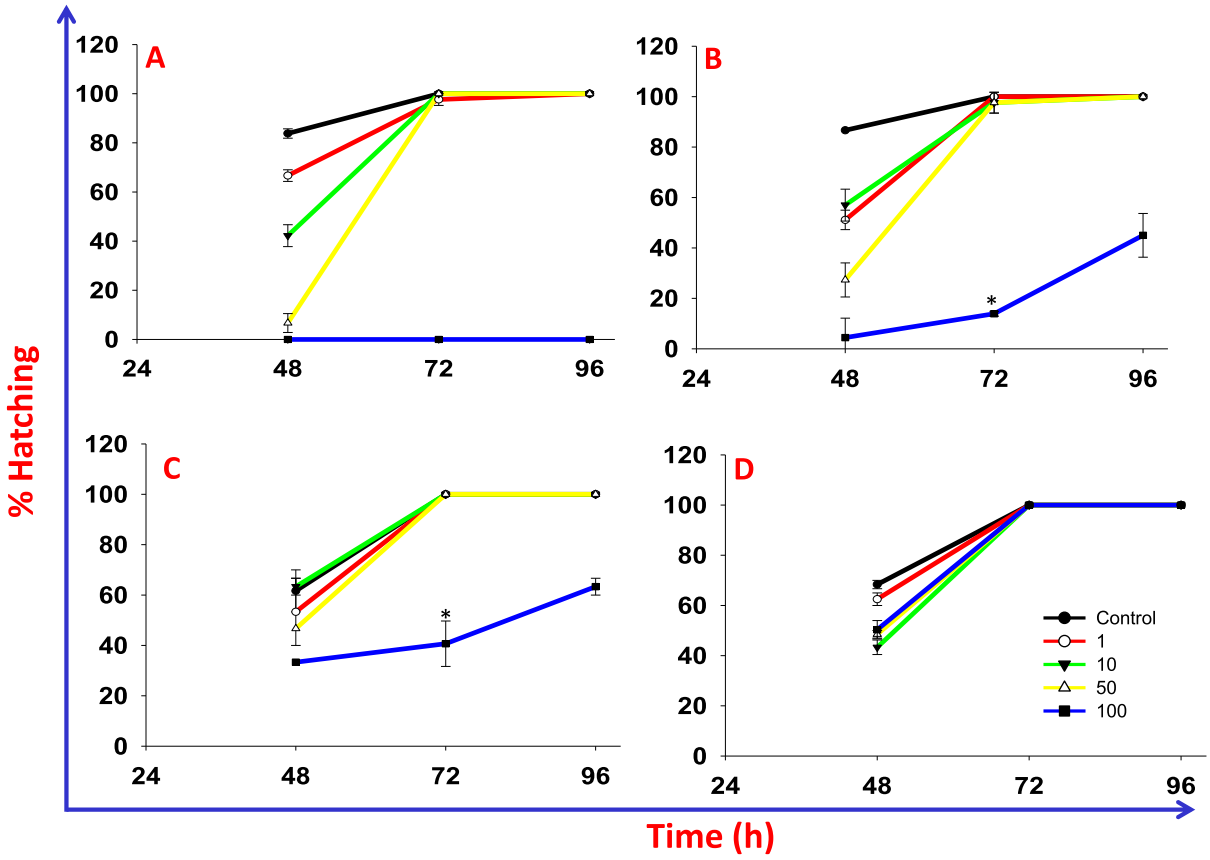

Fig. 7. Effects of humic acid (10 mg/L) and clay (10 mg/L) on the hatching success of zebrafish embryos after exposure to TiO_2 nanoparticles (1, 10, 50, 100 mg/L). (A) TiO_2 NPs (B) TiO_2 NPs + HA (C) TiO_2 NPs + Clay (D) TiO_2 NPs + HA + Clay. Data represent mean±SEM of three independent experiments. $^*P < 0.05$, when compared with control.

3.6. Reactive oxygen species (ROS) detection

The embryos are directly exposed to TiO_2 NPs after hatching. The TiO_2 NPs can significantly induce the oxidative stress in early developing embryos (Bar-Ilan, 2011; Bar-Ilan et al., 2012). The ROS generation by bare NPs was observed in concentration dependent manner in embryos. A significant quantitative increase in percent ROS generation was observed in zebrafish embryos after 72 h exposure to TiO_2 NPs. The fold increase in ROS generation was 10, 12 and 25 for 10, 50 and 100 mg/L bare TiO_2 NPs (Fig. 8A). Exposure to TiO_2 NPs generally elevates the level of ROS in zebrafish (Bar-Ilan, 2011; Bar-Ilan et al., 2012). The highest fluorescence intensity was observed in embryos exposed to bare TiO_2 NPs as compared to other combinations. However, no significant ROS generation was observed in presence of HA and HA + Clay. The ROS intensity increase was in order: TiO_2 NPs > TiO_2 NPs + Clay > TiO_2 NPs + HA + Clay > TiO_2 NPs + HA. Exposure to TiO_2 + HA and combination of HA and clay depicted lower ROS generation as compared to bare TiO_2 as observed for the survival rate of the embryos.

The ROS intensity remained unchanged in the 1 mg/L treated group, compared with the controls (Fig. 8). The induced level of ROS and oxidative stress can create several abnormalities in embryos (Yamashita, 2003).

3.7. Gene expression analysis

The survival rate, hatching delay and generation of ROS (Brun et al., 2018) play a key role in early developing embryos thus, several important genes involved in dorso-ventral axis formation, neural development, heart, intestine and jaw development were investigated to correlate the developmental abnormalities post exposure to TiO_2 NPs in presence and absence of abiotic factors. To compare genes expression from four different combinations: TiO_2 NPs, TiO_2 NPs + HA, TiO_2 NPs + Clay, TiO_2 NPs + HA + Clay, a panel of 12 genes and one housekeeping gene were selected from 96 hpf embryos (Fig. 9A–C). GAPDH is stably expressed in zebrafish and is used as housekeeping genes across all combinations. HA, Clay and HA + Clay without NPs were used as a control for different combinations.

Acvr1, Smad5 are expressed in cartilage and skeleton muscles. The normal growth and development of bones and muscles is controlled by Acvr1. Over expression of Acvr1 can induce alkaline phosphate activity and can lead to cartilage expansion and induce joint fusion which can enhance the chondrogenesis or dysregulation of BMP (bone morphogenetic protein) signaling pathway (Fukuda et al., 2009; Payne et al., 2001; Tylzanowski et al., 2001; Zhang et al., 2003). Further the BMP signaling pathway can activate the Smad pathway, which can result in the malformation of bones. The observed pattern of these gene expressions was 3 to 4 fold higher as compared to control in case of bare TiO_2 NPs exposure (Fig. 9A). However, in other exposure combinations the expression was either close to control (TiO_2 NPs + HA) or the change was not significant (TiO_2 NPs + HA + Clay; TiO_2 NPs + Clay; Fig. 9A). These results suggest that HA and combination of HA and clay suppress the bare NPs effect on the zebrafish embryos development with reference to bone formation.

Development of different cell types in vertebrate embryos starts with the pattern formation along the dorsal-ventral embryonic axis. The chordin (chrd) and szl genes can control dorsal-ventral patterning of zebrafish embryos by binding to ventralizing TGF-β protein. Szl requires chrd for the dorsalizing activity (Yabe et al., 2003). The reduced expression of chrd acts as BMP antagonist. The bare NPs and TiO_2 NPs + Clay reduced the chrd expression by 0.5 and 0.3 fold respectively.

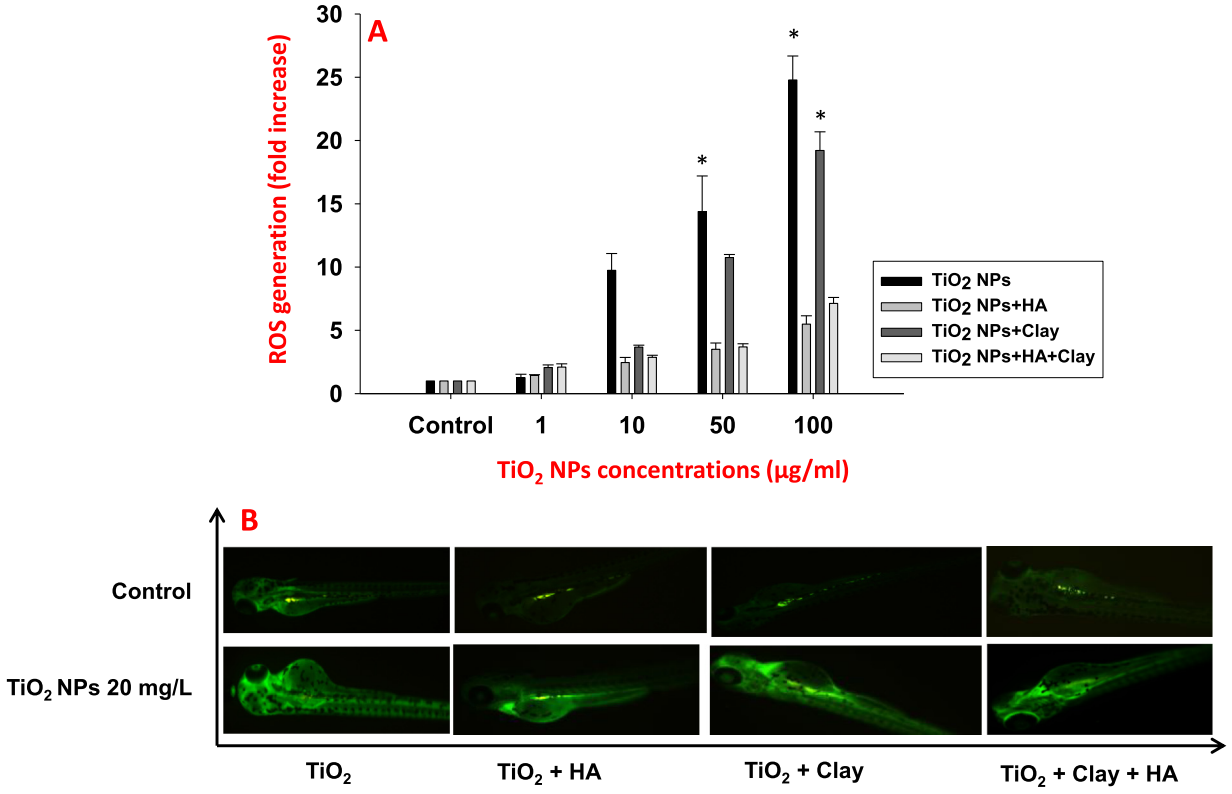

Fig. 8. Significant concentration-dependent increase in intracellular ROS using DCFDA dye (A) Bar graph depicts fold increase in ROS generation. Data represent mean±SEM of three independent experiments. *P < 0.05, when compared with control. (B) Zebrafish embryos treated with TiO_2 NPs (20 mg/L) in presence and absence of humic acid (10 mg/L) and clay (10 mg/L) and their combination. (Magnification X-400)

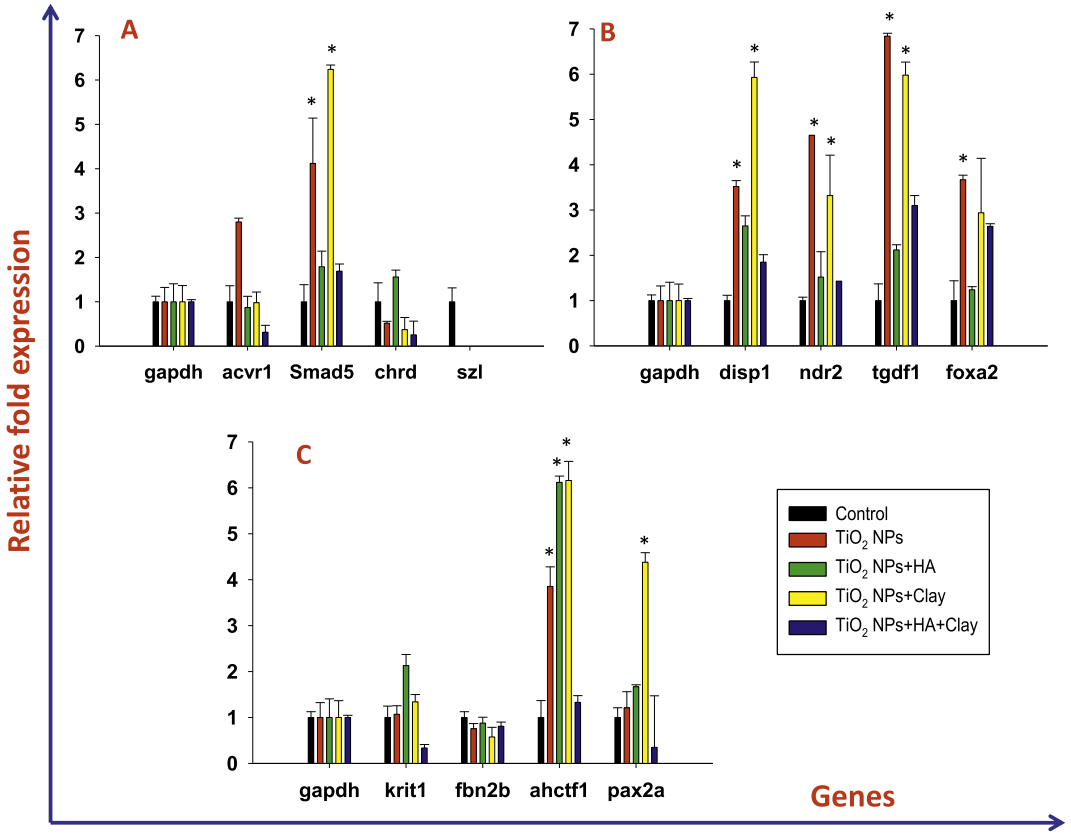

Fig. 9. Bar graph depicting fold change in relative gene expression of zebrafish embryos exposed to TiO_2 NPs (50 mg/L) in presence and absence of humic acid (10 mg/L) and clay (10 mg/L) and their combination at 96 h post fertilization (hpf). Data represent mean±SEM of three independent experiments. *P < 0.05, when compared with control.

The suppressed expression of chrd can lead to improper dorsalizing in embryos. The chrd expression by TiO_2 NPs + HA was 1.5 fold higher that indicates the normal dorsoventral development of embryos.

The normal Hedgehog (Hh) signaling pathway plays a critical role in craniofacial development in zebrafish embryos. The Hh-signaling pathway requires the disp1 (dispatched 1) gene for proper functioning. Mutation of disp1 gene causes under-developing jaw and pharyngeal arch skeleton of embryos. Disp1 relative gene expressions were 3.5, 2.6, 5.9 and 1.8 for TiO_2 NPs, TiO_2 NPs + HA, TiO_2 NPs + Clay and TiO_2 NPs + HA + Clay, respectively (Fig. 9B). The bare NPs and NPs with clay affected the jaw and pharyngeal arch skeleton of embryos but NPs with HA and NPs combined with HA and clay did not show any significant effect on the jaw formation. This is consistent with the observations for most of the other developmental genes especially those related to the structural development of the embryo.

Ndr2 and tgdf1 are important components for the formation of zebrafish anterior neural tube closure. These genes are part of Nodal signaling. Nodal signaling plays crucial role in many development stages of zebrafish (Halpern et al., 2003; Liang and Rubinstein, 2003; Schier and Shen, 2000; Schier and Talbot, 2003). Mutation of ndr2 and tdgf1 gene or nodal signaling pathway can do major defect in neural system including absence of hypothalamus (Harris and Juriloff, 2007). Our results showed the over expression of these genes exposed to bare NPs and NPs with clay particles, but NPs with HA and clay restored the normal functioning. The overall expressions of ndr2 and tgdf1 were 4.65 and 6.84 for TiO_2 NPs, 1.52 and 2.12 for TiO_2 NPs + HA, 3.32 and 5.98 for TiO_2 NPs + Clay and 1.43 and 3.1 for TiO_2 NPs + HA + Clay (Fig. 9B).

Foxa2 is associated in the development of floor plate in zebrafish. The floor plate is a specialized glial structure with secretory function that spans the rostral-caudal axis from the midbrain to the tail regions. The floor plate is one of first structures that differentiate in the developing nervous system of zebrafish (Higashijima et al., 1997). The overexpression of foxa2 can cause improper development floor plate which was observed for bare NPs exposure to embryos at 96 hpf. The expression of foxa2 exposed to TiO_2 NPs + Clay and TiO_2 NPs + HA + Clay were 2.7 and 2.6 respectively. However, TiO_2 NPs + HA showed similar expressions as control.

The effect of TiO_2 NPs in the development of different organs like heart, intestine and eye was also assessed by analyzing the genes involved in it. For cardiovascular and cardiac development Krit (formerly known as CCM1) and Fibrillin-2b (fbn2b) were selected. Krit1 interact with other proteins and stabilize the extracellular junctions. The decrease or loss of krit1 causes severe cardiovascular defect in zebrafish (Higashijima et al., 1997; Kleaveland et al., 2009; Mably et al., 2003, 2006; Whitehead et al., 2009; Yoruk et al., 2012; Zheng et al., 2010). Fibrillin-2b (fbn2b) is another gene associated with vasculogenesis and heart morphology of zebrafish was selected for the study. For most of the exposure combinations, no significant change in expression of krit1 and fbn2b was observed (Fig. 9C).

Pax2a is the member of Pax family protein that is expressed in developing visual system of zebrafish embryos. The observations depict that there was no significant change in pax2a expressions for bare NPs, TiO_2 NPs + HA, TiO_2 NPs + Clay and TiO_2 NPs + HA + Clay.

Ahctf1 gene is involved in early survival of embryos and also important for intestine formation. Over expression of this gene causes survival of embryo to larva stage (Chen et al., 2005). A significant increased expression of this gene was observed in the embryos exposed to TiO_2 NPs + HA and TiO_2 NPs + Clay. This observation supports the survival rate and hatching success results discussed previously (Fig. 9C).

The change in the expressions of several developmental genes exposed to bare NPs indicates their ability to induce malformation in the developing zebrafish embryos. However, it was also observed that the combination of HA and clay have the potential to restore the normal functioning of different developmental genes and can reduce the adverse effect of TiO_2 NPs.

4. Conclusions

Considering the nanoparticle exposure in presence of HA and clay in aqueous environment, the present data gives an insight towards the fate of nanoparticles in biological system. The presence of HA stabilized the ENP in MQ water as compared to bare ENMs or in presence of clay while the NPs in presence of HA + Clay showed stability intermediate of the HA and clay. However in zebrafish growth medium the high concentration of salts resulted in destabilization of NPs in presence or absence of abiotic factors. The presence of HA and clay affected the stability and dispersion of TiO_2 NPs in both MilliQ water and E3 medium. The HA and clay seemed to stabilize the NPs relative to bare TiO_2 NPs while the best stability was observed in presence of both HA and clay in E3 medium. The DLVO theory suggested that electrostatic stabilization does not play a major role in imparting stability to TiO_2 NPs. The abiotic factors seemed to directly affect the development of zebrafish embryos. HA and HA + Clay with TiO_2 NPs exhibit least toxicity in zebrafish embryos, possibly due to a combination of heteroaggregation and adsorption of HA that may have reduced the availability of nanoparticles. HA and clay minerals drastically reduces the effect of TiO_2 NPs on development of zebrafish embryos. Bare TiO_2 NPs and TiO_2 NPs + clay significantly altered the expression of genes involved in development of dorsoventral axis and neural network of zebrafish embryos. However, the presence of HA and HA with clay showed protective effect on developmental genes. A combination of HA and clay in E3 medium is closer to the actual aqueous environment and thus it is important to know how ENMs behave in actual aqueous environment for designing sustainable ENMs. Based on the observation made in laboratory scale microcosm, it can be suggested that HA and clay can act as naturally existing nonhazardous agents to remove TiO_2 nanoparticle contamination from water regardless of their different mechanism of removal. Further studies are required to understand the actual mechanism by which the combination of HA and clay is reducing the toxicity of ENMs through reduced bioavailability or transport or internalization or a combination of all. Though our study demonstrated the combined effect of HA and clay on TiO_2 NPs at the laboratory scale, the real environmental situation is much more complex, thus the detail study of contamination removal has to be investigated further.

Declaration of competing interest

There are no conflicts to declare.

Acknowledgment

Funding received from IMPRINT - Ministry of Human Resource Development, Government of India for the project “Advanced nanotracers for product life cycle assessment and product monitoring”, the Department of Biotechnology, Government of India under the project “NanoToF: Toxicological evaluation and risk assessment on Nanomaterials in Food” (grant number BT/PR10414/PFN/20/961/2014) and DST SERB Project “Nanosensors for the Detection of Food Adulterants and Contaminants” (grant number EMR/2016/005286) is gratefully acknowledged. Financial assistance by The Gujarat Institute for Chemical Technology (GICT) for the establishment of a facility for environmental risk assessment of chemicals and nanomaterials is also acknowledged. Krupa Kansara would like to acknowledge Council of Scientific & Industrial Research for providing fellowship.

Appendix A. Supplementary data

Supplementary data to this article can be found online at https://doi.org/10.1016/j.scitotenv.2019.134133.

References

Ates, M., Daniels, J., Arslan, Z., Farah, I.O., 2013. Effects of aqueous suspensions of titanium dioxide nanoparticles on Artemia salina: assessment of nanoparticle aggregation, accumulation, and toxicity. Environ. Monit. Assess. 185, 3339–3348.

Bai, W., Zhang, Z., Tian, W., He, X., Ma, Y., Zhao, Y., et al., 2010. Toxicity of zinc oxide nanoparticles to zebrafish embryo: a physicochemical study of toxicity mechanism. J. Nanopart. Res. 12, 1645–1654.

Bar-Ilan, O., 2011. Toxicity of Metal and Metal Oxide Nanoparticles in Developing Zebrafish. University of Wisconsin–Madison.

Bar-Ilan, O., Louis, K.M., Yang, S.P., Pedersen, J.A., Hamers, R.J., Peterson, R.E., et al., 2012. Titanium dioxide nanoparticles produce phototoxicity in the developing zebrafish. Nanotoxicology 6, 670–679.

Bar-Ilan, O., Chuang, C.C., Schwahn, D.J., Yang, S., Joshi, S., Pedersen, J.A., et al., 2013. TiO2 nanoparticle exposure and illumination during zebrafish development: mortality at parts per billion concentrations. Environ. Sci. Technol. 47, 4726–4733.

Bhuvaneshwari, M., Thiagarajan, V., Nemade, P., Chandrasekaran, N., Mukherjee, A., 2018. Toxicity and trophic transfer of P25 TiO2 NPs from Dunaliella salina to Artemia salina: effect of dietary and waterborne exposure. Environ. Res. 160, 39–46.

Brun, N.R., Koch, B.E., Varela, M., Peijnenburg, W.J., Spaink, H.P., Vijver, M.G., 2018. Nanoparticles induce dermal and intestinal innate immune system responses in zebrafish embryos. Environ. Sci.: Nano 5, 904–916.

Buffle, J., Wilkinson, K.J., Stoll, S., Filella, M., Zhang, J., 1998. A generalized description of aquatic colloidal interactions: the three-colloidal component approach. Environ. Sci. Technol. 32, 2887–2899.

Cai, L., Tong, M., Wang, X., Kim, H., 2014. Influence of clay particles on the transport and retention of titanium dioxide nanoparticles in quartz sand. Environ. Sci. Technol. 48, 7323–7332.

Chen, J., Ruan, H., Ng, S.M., Gao, C., Soo, H.M., Wu, W., et al., 2005. Loss of function of def selectively up-regulates Delta113p53 expression to arrest expansion growth of digestive organs in zebrafish. Genes Dev. 19, 2900–2911.

Chen, J., Xiu, Z., Lowry, G.V., Alvarez, P.J., 2011a. Effect of natural organic matter on toxicity and reactivity of nano-scale zero-valent iron. Water Res. 45, 1995–2001.

Chen, K.L., Elimelech, M., 2006. Aggregation and deposition kinetics of fullerene (C60) nanoparticles. Langmuir 22, 10994–11001.

Chen, T.H., Lin, C.Y., Tseng, M.C., 2011b. Behavioral effects of titanium dioxide nanoparticles on larval zebrafish (Danio rerio). Mar. Pollut. Bull. 63, 303–308.

Cheng, H., Yan, W., Wu, Q., Lu, J., Liu, C., Hung, T.-C., et al., 2018. Adverse reproductive performance in zebrafish with increased bioconcentration of microcystin-LR in the presence of titanium dioxide nanoparticles. Environ. Sci.: Nano 5, 1208–1217.

Cheng, J., Flahaut, E., Cheng, S.H., 2007. Effect of carbon nanotubes on developing zebrafish (Danio rerio) embryos. Environ. Toxicol. Chem. 26, 708–716.

de Melo, B.A., Motta, F.L., Santana, M.H., 2016. Humic acids: structural properties and multiple functionalities for novel technological developments. Mater. Sci. Eng. C Mater. Biol. Appl. 62, 967–974.

Deng, J., Yu, L., Liu, C., Yu, K., Shi, X., Yeung, L.W., et al., 2009. Hexabromocyclododecane-induced developmental toxicity and apoptosis in zebrafish embryos. Aquat. Toxicol. 93, 29–36.

Devi, G.P., Ahmed, K.B., Varsha, M.K., Shrijha, B.S., Lal, K.K., Anbazhagan, V., et al., 2015. Sulfidation of silver nanoparticle reduces its toxicity in zebrafish. Aquat. Toxicol. 158, 149–156.

Domingos, R.F., Baalousha, M.A., Ju-Nam, Y., Reid, M.M., Tufenkji, N., Lead, J.R., et al., 2009a. Characterizing manufactured nanoparticles in the environment: multimethod determination of particle sizes. Environ. Sci. Technol. 43, 7277–7284.

Domingos, R.F., Tufenkji, N., Wilkinson, K.J., 2009b. Aggregation of titanium dioxide nanoparticles: role of a fulvic acid. Environ. Sci. Technol. 43, 1282–1286.

Elimelech, M., Gregory, J., Jia, X., 2013. Particle Deposition and Aggregation: Measurement, Modelling and Simulation. Butterworth-Heinemann.

Fabrega, J., Fawcett, S.R., Renshaw, J.C., Lead, J.R., 2009. Silver nanoparticle impact on bacterial growth: effect of pH, concentration, and organic matter. Environ. Sci. Technol. 43, 7285–7290.

Faria, M., Navas, J.M., Raldua, D., Soares, A.M., Barata, C., 2014. Oxidative stress effects of titanium dioxide nanoparticle aggregates in zebrafish embryos. Sci. Total Environ. 470-471, 379–389.

Filho Jde, S., Matsubara, E.Y., Franchi, L.P., Martins, I.P., Rivera, L.M., Rosolen, J.M., et al., 2014. Evaluation of carbon nanotubes network toxicity in zebrafish (Danio rerio) model. Environ. Res. 134, 9–16.

French, R.A., Jacobson, A.R., Kim, B., Isley, S.L., Penn, R.L., Baveye, P.C., 2009. Influence of ionic strength, pH, and cation valence on aggregation kinetics of titanium dioxide nanoparticles. Environ. Sci. Technol. 43, 1354–1359.

Fukuda, T., Kohda, M., Kanomata, K., Nojima, J., Nakamura, A., Kamizono, J., et al., 2009. Constitutively activated ALK2 and increased SMAD1/5 cooperatively induce bone morphogenetic protein signaling in fibrodysplasia ossificans progressiva. J. Biol. Chem. 284, 7149–7156.

Gao, J., Youn, S., Hovsepyan, A., Llaneza, V.L., Wang, Y., Bitton, G., et al., 2009. Dispersion and toxicity of selected manufactured nanomaterials in natural river water samples: effects of water chemical composition. Environ. Sci. Technol. 43, 3322–3328.

Gao, J., Powers, K., Wang, Y., Zhou, H., Roberts, S.M., Moudgil, B.M., et al., 2012. Influence of Suwannee River humic acid on particle properties and toxicity of silver nanoparticles. Chemosphere 89, 96–101.

George, S., Xia, T., Rallo, R., Zhao, Y., Ji, Z., Lin, S., et al., 2011. Use of a high-throughput screening approach coupled with in vivo zebrafish embryo screening to develop hazard ranking for engineered nanomaterials. ACS Nano 5, 1805–1817.

Guo, Y., Chen, L., Wu, J., Hua, J., Yang, L., Wang, Q., et al., 2019. Parental co-exposure to bisphenol A and nano-TiO2 causes thyroid endocrine disruption and developmental neurotoxicity in zebrafish offspring. Sci. Total Environ. 650, 557–565.

Gupta, G.S., Dhawan, A., Shanker, R., 2016a. Montmorillonite clay alters toxicity of silver nanoparticles in zebrafish (Danio rerio) eleutheroembryo. Chemosphere 163, 242–251.

Gupta, G.S., Kumar, A., Shanker, R., Dhawan, A., 2016b. Assessment of agglomeration, co-sedimentation and trophic transfer of titanium dioxide nanoparticles in a laboratory-scale predator-prey model system. Sci. Rep. 6, 31422.

Gupta, G.S., Kumar, A., Senapati, V.A., Pandey, A.K., Shanker, R., Dhawan, A., 2017. Laboratory scale microbial food chain to study bioaccumulation, biomagnification, and ecotoxicity of cadmium telluride quantum dots. Environ. Sci. Technol. 51, 1695–1706.

Gupta, G.S., Kansara, K., Shah, H., Rathod, R., Valecha, D., Gogisetty, S., et al., 2019. Impact of humic acid on the fate and toxicity of titanium dioxide nanoparticles in Tetrahymena pyriformis and zebrafish embryos. Nanoscale Advances 1, 219–227.

Hajdú, A., Illés, E., Tombácz, E., Borbáth, I., 2009. Surface charging, polyanionic coating and colloid stability of magnetite nanoparticles. Colloids Surf. A Physicochem. Eng. Asp. 347, 104–108.

Halpern, M.E., Liang, J.O., Gamse, J.T., 2003. Leaning to the left: laterality in the zebrafish forebrain. Trends Neurosci. 26, 308–313.

Harris, M.J., Juriloff, D.M., 2007. Mouse mutants with neural tube closure defects and their role in understanding human neural tube defects. Birth Defects Res. A Clin. Mol. Teratol. 79, 187–210.

Higashijima, S., Nose, A., Eguchi, G., Hotta, Y., Okamoto, H., 1997. Mindin/F-spondin family: novel ECM proteins expressed in the zebrafish embryonic axis. Dev. Biol. 192, 211–227.

Howe, K., Clark, M.D., Torroja, C.F., Torrance, J., Berthelot, C., Muffato, M., et al., 2013. The zebrafish reference genome sequence and its relationship to the human genome. Nature 496, 498.

Jayalath, S., Wu, H., Larsen, S.C., Grassian, V.H., 2018. Surface adsorption of Suwannee River humic acid on TiO2 nanoparticles: a study of pH and particle size. Langmuir 34, 3136–3145.

Keller, A.A., Lazareva, A., 2013. Predicted releases of engineered nanomaterials: from global to regional to local. Environ. Sci. Technol. Lett. 1, 65–70.

Keller, A.A., Wang, H., Zhou, D., Lenihan, H.S., Cherr, G., Cardinale, B.J., et al., 2010. Stability and aggregation of metal oxide nanoparticles in natural aqueous matrices. Environ. Sci. Technol. 44, 1962–1967.

Kleaveland, B., Zheng, X., Liu, J.J., Blum, Y., Tung, J.J., Zou, Z., et al., 2009. Regulation of cardiovascular development and integrity by the heart of glass-cerebral cavernous malformation protein pathway. Nat. Med. 15, 169–176.

Labille, J., Harns, C., Bottero, J.Y., Brant, J., 2015. Heteroaggregation of titanium dioxide nanoparticles with natural clay colloids. Environ. Sci. Technol. 49, 6608–6616.

Lagaly, G., Ziesmer, S., 2003. Colloid chemistry of clay minerals: the coagulation of montmorillonite dispersions. Adv. Colloid Interf. Sci. 100, 105–128.

Lee, S., Kim, K., Shon, H., Kim, S.D., Cho, J., 2011. Biotoxicity of nanoparticles: effect of natural organic matter. J. Nanopart. Res. 13, 3051–3061.

Levard, C., Hotze, E.M., Colman, B.P., Dale, A.L., Truong, L., Yang, X.Y., et al., 2013. Sulfidation of silver nanoparticles: natural antidote to their toxicity. Environ. Sci. Technol. 47, 13440–13448.

Liang, J.O., Rubinstein, A.L., 2003. Patterning of the zebrafish embryo by nodal signals. Curr. Top. Dev. Biol. 55, 143–171.

Lin, S., Zhao, Y., Ji, Z., Ear, J., Chang, C.H., Zhang, H., et al., 2013. Zebrafish high-throughput screening to study the impact of dissolvable metal oxide nanoparticles on the hatching enzyme, ZHE1. Small 9, 1776–1785.

Loosli, F., Le Coustumer, P., Stoll, S., 2013. TiO2 nanoparticles aggregation and disaggregation in presence of alginate and Suwannee River humic acids. pH and concentration effects on nanoparticle stability. Water Res. 47, 6052–6063.

Mably, J.D., Mohideen, M.A., Burns, C.G., Chen, J.N., Fishman, M.C., 2003. Heart of glass regulates the concentric growth of the heart in zebrafish. Curr. Biol. 13, 2138–2147.

Mably, J.D., Chuang, L.P., Serluca, F.C., Mohideen, M.A., Chen, J.N., Fishman, M.C., 2006. Santa and valentine pattern concentric growth of cardiac myocardium in the zebrafish. Development 133, 3139–3146.

Mahmoudi, M., Lynch, I., Ejtehadi, M.R., Monopoli, M.P., Bombelli, F.B., Laurent, S., 2011. Protein− nanoparticle interactions: opportunities and challenges. Chem. Rev. 111, 5610–5637.

Massarsky, A., Dupuis, L., Taylor, J., Eisa-Beygi, S., Strek, L., Trudeau, V.L., et al., 2013. Assessment of nanosilver toxicity during zebrafish (Danio rerio) development. Chemosphere 92, 59–66.

Ong, K.J., Zhao, X., Thistle, M.E., Maccormack, T.J., Clark, R.J., Ma, G., et al., 2014. Mechanistic insights into the effect of nanoparticles on zebrafish hatch. Nanotoxicology 8, 295–304.

Payne, T.L., Postlethwait, J.H., Yelick, P.C., 2001. Functional characterization and genetic mapping of alk8. Mech. Dev. 100, 275–289.

Pertusatti, J., Prado, A.G., 2007. Buffer capacity of humic acid: thermodynamic approach. J. Colloid Interface Sci. 314, 484–489.

Radniecki, T.S., Stankus, D.P., Neigh, A., Nason, J.A., Semprini, L., 2011. Influence of liberated silver from silver nanoparticles on nitrification inhibition of Nitrosomonas europaea. Chemosphere 85, 43–49.

Renieri, E.A., Sfakianakis, D.G., Alegakis, A.A., Safenkova, I.V., Buha, A., Matovic, V., et al., 2017. Nonlinear responses to waterborne cadmium exposure in zebrafish. An in vivo study. Environ. Res. 157, 173–181.

Robichaud, C.O., Uyar, A.E., Darby, M.R., Zucker, L.G., Wiesner, M.R., 2009. Estimates of Upper Bounds and Trends in Nano-TiO2 Production as a Basis for Exposure Assessment. ACS Publications.

Romanello, M.B., Fidalgo de Cortalezzi, M.M., 2013. An experimental study on the aggregation of TiO2 nanoparticles under environmentally relevant conditions. Water Res. 47, 3887–3898.

Sajjadi, H., Modaressi, A., Magri, P., Domańska, U., Sindt, M., Mieloszynski, J.-L., et al., 2013. Aggregation of nanoparticles in aqueous solutions of ionic liquids. J. Mol. Liq. 186, 1–6.
Schier, A.F., Shen, M.M., 2000. Nodal signalling in vertebrate development. Nature 403, 385.
Schier, A.F., Talbot, W.S., 2003. Nodal signaling and the zebrafish organizer. Int. J. Dev. Biol. 45, 289–297.
Tylzanowski, P., Verschueren, K., Huylebroeck, D., Luyten, F.P., 2001. Smad-interacting protein 1 is a repressor of liver/bone/kidney alkaline phosphatase transcription in bone morphogenetic protein-induced osteogenic differentiation of C2C12 cells. J. Biol. Chem. 276, 40001–40007.
Wang, H., Dong, Y.N., Zhu, M., Li, X., Keller, A.A., Wang, T., et al., 2015. Heteroaggregation of engineered nanoparticles and kaolin clays in aqueous environments. Water Res. 80, 130–138.
Weir, A., Westerhoff, P., Fabricius, L., Hristovski, K., von Goetz, N., 2012. Titanium dioxide nanoparticles in food and personal care products. Environ. Sci. Technol. 46, 2242–2250.
Westerfield, M., 2007. The Zebrafish Book: A Guide for the Laboratory Use of Zebrafish Danio ("Brachydanio rerio"). University of Oregon.
Whitehead, K.J., Chan, A.C., Navankasattusas, S., Koh, W., London, N.R., Ling, J., et al., 2009. The cerebral cavernous malformation signaling pathway promotes vascular integrity via Rho GTPases. Nat. Med. 15, 177–184.
Wilkinson, K.J., Joz-Roland, A., Buffle, J., 1997. Different roles of pedogenic fulvic acids and aquagenic biopolymers on colloid aggregation and stability in freshwaters. Limnol. Oceanogr. 42, 1714–1724.
Wu, M., Xu, H., Shen, Y., Qiu, W., Yang, M., 2011. Oxidative stress in zebrafish embryos induced by short-term exposure to bisphenol A, nonylphenol, and their mixture. Environ. Toxicol. Chem. 30, 2335–2341.
Yabe, T., Shimizu, T., Muraoka, O., Bae, Y.K., Hirata, T., Nojima, H., et al., 2003. Ogon/secreted frizzled functions as a negative feedback regulator of Bmp signaling. Development 130, 2705–2716.
Yamashita, M., 2003. Apoptosis in zebrafish development. Comp. Biochem. Physiol. B: Biochem. Mol. Biol. 136, 731–742.
Yang, S.P., Bar-Ilan, O., Peterson, R.E., Heideman, W., Hamers, R.J., Pedersen, J.A., 2013. Influence of humic acid on titanium dioxide nanoparticle toxicity to developing zebrafish. Environ. Sci. Technol. 47, 4718–4725.
Yoruk, B., Gillers, B.S., Chi, N.C., Scott, I.C., 2012. Ccm3 functions in a manner distinct from Ccm1 and Ccm2 in a zebrafish model of CCM vascular disease. Dev. Biol. 362, 121–131.
Zhang, D., Schwarz, E.M., Rosier, R.N., Zuscik, M.J., Puzas, J.E., O'Keefe, R.J., 2003. ALK2 functions as a BMP type I receptor and induces Indian hedgehog in chondrocytes during skeletal development. J. Bone Miner. Res. 18, 1593–1604.
Zheng, X., Xu, C., Di Lorenzo, A., Kleaveland, B., Zou, Z., Seiler, C., et al., 2010. CCM3 signaling through sterile 20-like kinases plays an essential role during zebrafish cardiovascular development and cerebral cavernous malformations. J. Clin. Invest. 120, 2795–2804.
Zhou, D., Abdel-Fattah, A.I., Keller, A.A., 2012. Clay particles destabilize engineered nanoparticles in aqueous environments. Environ. Sci. Technol. 46, 7520–7526.